

Galactic Magnetic Field Bias on Inferences from UHECR Data

B. Eichmann,^{a,1} T. Winchen^b

^aRuhr Astroparticle and Plasma Physics Center (RAPP Center), Ruhr-Universität Bochum, Institut für Theoretische Physik IV, 44780 Bochum, Germany

^bAstrophysical Institute, Vrije Universiteit Brussel (VUB), Pleinlaan 2, 1050 Brussels, Belgium

Now at Max-Planck-Institut für Radioastronomie (MPIfR), Auf dem Hügel 69, 53121 Bonn, Germany

E-mail: eiche@tp4.rub.de, tobias.winchen@rwth-aachen.de

Abstract. A consequence of Liouville’s theorem indicates that the recently observed large scale anisotropy in the arrival direction of Ultra-High-Energy Cosmic Rays (UHECRs) cannot be produced by the Galactic magnetic field, thus this anisotropy already needs to be present outside our Galaxy. But in this case, the observed energy spectrum and composition of UHECRs differs from the one outside of the Milky Way, due to the suppression or the amplification of the UHECR flux from certain directions by the Galactic magnetic field. In this work, we investigate this effect for the case of a dipole and a quadrupole anisotropy, respectively, for the widely-used JF12 magnetic field model. We investigate boundaries on the maximal amplitude of the observed anisotropy and the maximal charge number of UHECRs. Furthermore, the flux modification is discussed in the light of the Auger data on the recent dipole and also the chemical composition. We find that this modification effect yields a modification of the observed flux of up to $\sim 10\%$ for the investigated magnetic field model and the observed dipole, in particular for a heavy chemical composition of UHECRs as suggested by the ‘EPOS-LHC’ model.

¹Corresponding author.

Contents

1	Introduction	1
2	Method	2
3	General bias	4
3.1	Anisotropy amplitude	4
3.2	Total flux bias for a dipole anisotropy	6
3.2.1	An ideal observer	6
3.2.2	Difference between Auger and TA	6
3.3	Total flux bias for a quadrupole anisotropy	7
4	Bias based on the Auger data	7
4.1	Total flux in case of the Auger dipole	8
4.2	Constraints on the chemical composition	9
5	Conclusions	10
	Bibliography	12

1 Introduction

Ultra-high energy cosmic rays (UHECRs) are believed to be charged nuclei that penetrate Earth’s atmosphere with energies above about 1 EeV that are likely accelerated in powerful extragalactic objects [1]. In principle, this reveals the possibility for cosmic ray astronomy, however, UHECRs get deflected by the magnetic fields inside and outside our Galaxy. Under certain constraints — that seem satisfied in the case of UHECRs — the magnetic fields cannot introduce anisotropies, according to Liouville’s theorem. An isotropic cosmic ray distribution outside the Milky Way has to be isotropic at Earth, and the properties of the UHECRs like the energy spectrum do not change. However, the arrival directions of UHECR show clear evidence of a dipole anisotropy [2] and thus also the observed properties of the UHECR flux can get modified by the Galactic magnetic field compared to the extragalactic flux used for inferences on UHECR sources [3]. Thus, inferences from UHECR data are impacted by the assumed magnetic fields. Unfortunately the Galactic magnetic field is not well known and the model by Jansson and Farrar [4], hereafter referred to as JF12, which is widely used in the cosmic ray community, fails to describe all available data [5–7].

A first view on this effect for the JF12 model [8] has shown that the modification depends significantly on the dipole direction and its amplitude, and that especially above some tens of EeV, the change by the Galactic magnetic field is expected to be negligible compared to the observational uncertainties. However, in this study neither the observed change of the dipole strength and direction, nor the increasing heaviness of the UHECR composition or the limited field of view of the experiments have been taken into account. This work clarifies if under consideration of the data of the Pierre Auger Observatory, the UHECR spectrum at Earth is significantly different from the one outside our Galaxy assuming the JF12 model and dipole as well as quadrupole anisotropies. Further, it discusses if this effect is able to resolve the

puzzling discrepancies of the UHECR flux [9] between the Pierre Auger Observatory (Auger) and the Telescope Array (TA) experiments.

2 Method

To investigate the impact of the Galactic magnetic field on UHECRs simulations of their propagation are required. Unfortunately, forward simulation of the propagation through the galaxy is challenging, since the probability to hit the Earth by chance becomes extremely small — about $1 : 10^{30}$. However, as the propagation distance of UHECRs through the Galactic environment is comparatively small with respect to the length scale of stochastic energy losses, the cosmic ray energy has hardly changed from the edge of our Galaxy to Earth. Thus, the arrival direction at Earth depends only on the initial phase-space coordinates of the particle and its rigidity $R = E/(eZ)$ given by the ratio of the energy E over the charge eZ of the particle, according to the Lorentz force. The effect of the magnetic field on the cosmic ray arrival direction can thus be described as lens [10] that transforms the cosmic ray arrival directions from outside the Milky Way to Earth.

An efficient technique to create such a Galactic lens in simulations is the so-called back-tracking method, where anti-particles are propagated backwards to obtain the trajectories of the regular particles that hit the Earth [11]. Here, all trajectories that end up at the edge of the Galaxy yield possible arrival directions at Earth. The lens can be described as set of matrices $\mathcal{L}(\vec{r}, R)$ of the density of trajectories, that transforms the distribution $M_0(R, \vec{r})$ of arrival directions \vec{r} from outside our Galaxy to Earth dependent on the particles' rigidity R to the observed distribution at Earth $M(\vec{r}, R) = \mathcal{L}(\vec{r}, R) \cdot M_0(\vec{r})$. To obtain matrices of finite size, the directions are binned into equal area pixels following the HEALPix scheme [12]. Simulation of the particle trajectories for the lens as well as its application to the model maps are performed using the publicly available CRPropa3¹ code [13].

In this work, the Galactic lens is generated from about $256 \times 49 \times 152$ isotropically emitted particles for each of 200 logarithmically binned rigidities between 0.1 EV and 10^3 EV. These numbers enable sufficient statistics for a resolution of the lens of about 1 degree. Here, we use predominantly the JF12 model with three different coherence lengths λ of the turbulent component of the magnetic field. Since λ is expected to be about a fifth of the maximal length scale of the turbulent system, we use $\lambda \in \{10, 60, 100\}$ pc.

In order to construct a certain distribution of arrival directions outside our Galaxy, we use Healpy² in order to generate a map M_0 of 49×152 pixels with a certain value. In the case of an ideal dipole anisotropy with a dipole \vec{d} these values are given by

$$M_0(\vec{r}) = 1 + \vec{d} \cdot \vec{r}, \quad (2.1)$$

where \vec{r} denotes the spatial direction of a given pixel and the first term represents the normalised monopole. Note that the dipole amplitude is given by $d = |\vec{d}|$. In the case of an ideal quadrupole $\tilde{Q}_{ij} = 3q_i q_j - \delta_{ij}$ without any dipole anisotropy, the distribution is determined by

$$M_0(\vec{r}) = 1 + \frac{1}{2} \sum_{i,j} Q_{ij} r_i r_j, \quad (2.2)$$

¹<https://crpropa.desy.de>

²<https://healpy.readthedocs.io>

where the normalized quadrupole Q_{ij} is used, that provides an average quadrupole amplitude $Q = \sqrt{\sum_{ij} Q_{ij}^2 / 9}$.

Note, that the unit vector \vec{q} defines the direction of one of the two maxima of the quadrupole distribution and the scalar Q determines the amplitude. Thus, the maximal value of the distribution M_0 yields $1+d$ for the dipole and $1+Q$ for the quadrupole, respectively. We only consider a symmetric quadrupole to keep the number of studied variables manageable, i.e. the eigenvalues of Q_{ij} are given by $\lambda_- = \lambda_0 = -\lambda_+/2$. So, only the strength of the quadrupole amplitude Q will be varied in the following.

In the case of an ideal detector the Galactic modification of the total UHECR flux is given by

$$\Delta F = \frac{\sum M}{\sum M_0} - 1. \quad (2.3)$$

Furthermore, the redistribution of cosmic rays by the Galactic magnetic field leads to a modification of the strength and direction of the individual components of the anisotropy. Here, the amplitude of the dipole and the quadrupole, respectively, is proportional to its corresponding coefficient C_1 and C_2 , respectively, of the spherical harmonics according to

$$d = \sqrt{\frac{9C_1}{C_0}} \text{ and } Q = \sqrt{\frac{50C_2}{3C_0}}, \quad (2.4)$$

where C_0 denotes the coefficient of the monopole. Hence, we compare the resulting coefficient $C_l(M)$ after the lensing with the coefficient $C_l(M_0)$ before the lensing to obtain a measure of the change of the anisotropy amplitude. So, the modification of the anisotropy amplitude is given by

$$\Delta d = \sqrt{\frac{C_1(M) C_0(M_0)}{C_1(M_0) C_0(M)}} - 1, \text{ and } \Delta Q = \sqrt{\frac{C_2(M) C_0(M_0)}{C_2(M_0) C_0(M)}} - 1, \quad (2.5)$$

respectively. In addition, the regular component of the Galactic magnetic field also changes the direction of the anisotropy. To account for this effect in case of a dipole, we use the Galactic lens to determine the angular change

$$\vec{\Delta}_d = \arccos\left(\vec{d} \cdot \vec{d}_{\text{obs}} / |\vec{d}_{\text{obs}}|\right) \quad (2.6)$$

of the direction of the dipole from outside the Galaxy to Earth. In the case of the quadrupole, the correlation of the directions of the maximas outside the Galaxy to the ones at Earth becomes indistinct — in particular for strong direction changes that already occur at $R \lesssim 10 \text{ EV}$. In addition, the lens also introduce anisotropies of different order, which makes a naive correlation ambiguous. Therefore, we only include the change the dipole direction in this work in particular as no quadrupole has been observed yet.

The lens \mathcal{L} is build from the backtracking of anti-particles into 49 152 equidistant directions, so that not necessarily every direction outside the Galaxy hits the Earth. Therefore, it is not trivial to invert the lens \mathcal{L} and we choose a more simple approach, where we build a rigidity dependent correlation scheme that relates the corresponding dipole direction at Earth for 3072 equidistant dipole direction outside the Galaxy. So, for an arbitrary dipole direction at Earth, we use the one that possesses the smallest angle with respect to this direction.

In order to account for the limited field of view of the UHECR observatories, we use the declination δ dependent directional exposure [14]

$$\omega(\delta) = \cos(\lambda_i) \cos(\delta) \sin(\arccos(\xi)) + \arccos(\xi) \sin(\lambda_i) \sin(\delta), \quad (2.7)$$

with

$$\xi(\delta) = \frac{\cos(\alpha_i) - \sin(\lambda_i) \sin(\delta)}{\cos(\lambda_i) \cos(\delta)}. \quad (2.8)$$

Here, λ_i denotes the latitude of the considered experiment, hence, $\lambda_{\text{Auger}} = -35.25^\circ$ for Auger and $\lambda_{\text{TA}} = 39.30^\circ$ for TA. Further, α_i is the maximal zenith angle of the arriving cosmic ray that is taken into account by the experiment. Although, α_i slightly depends on the energy, we use a constant value of $\alpha_{\text{Auger}} = 80^\circ$ and $\alpha_{\text{TA}} = 45^\circ$, respectively. Since the observatories already account for this exposure dependence in their spectrum measurement, we only have to consider the different field of views given by the acceptance

$$a(\delta) = \begin{cases} 4\pi/\Omega_i & \text{for } \omega(\delta) \neq 0 \\ 0 & \text{for } \omega(\delta) = 0, \end{cases} \quad (2.9)$$

where Ω_i denotes the non-vanishing solid angle of the detector's field of view, in order to obtain the detector dependent UHECR flux. Thus, each pixel of the given map has a certain declination dependent acceptance $a(\delta)$, so that $M' = M \cdot a(\delta)$, and $M'_0 = M_0 \cdot a(\delta)$ yields the resulting distribution at the observatories with and without the impact by the Galactic magnetic field, respectively. Hence, $\Delta F_i = \sum M' / \sum M'_0 - 1$ provides the Galactic modification of the total UHECR flux dependent on the observatories field of view.

3 General bias

In the following, we use the JF12 model of the Galactic magnetic field with a turbulent coherence length of $\lambda = 60$ pc, unless otherwise stated. Hereby, we evaluated 3072 equidistant anisotropy directions at Earth which yields a resolution of $< 5^\circ$.

3.1 Anisotropy amplitude

The Galactic lens transforms the cosmic ray distribution from outside our Galaxy to Earth, however, only the characteristics of the distribution at Earth are accessible via experiments. Therefore, we first investigate the change of the anisotropy — direction and amplitude — by the Galactic magnetic field. In general, the directions of the dipole are significantly shifted for some directions at rigidities $\lesssim 10$ EV, as shown in the left Fig. 1. According to the middle Fig. 1, also the dipole amplitude decreases significantly at these rigidities, and thus, the Galactic magnetic field introduces anisotropies of higher order. In the case of the quadrupole, we obtain similar behaviour, but the amplitude is in principle reduced more by almost a factor two. The change of the dipole direction hardly depends on the coherence length λ of the turbulent magnetic field component, though in general the anisotropy amplitude decreases for an increasing λ . Hence, a change from $\lambda = 10$ pc to $\lambda = 100$ pc can increase the suppression by about 20 % at a few EV. At $R \lesssim 1$ EV the dipole completely vanishes for some directions leading to a sudden decrease of the maximal value of $\vec{\Delta}_d$, as the change of direction almost coincides with the change of amplitude — see Fig. 2. Here, predominantly the narrow band of directions, that is shown in the left Fig. 2, still holds a non-vanishing dipole providing a maximal change of direction of only about 90° .

In the case of the dipole anisotropy, Fig. 2 show those dipole directions at Earth, that are biased the most by the Galactic magnetic field. At a few EeV the patterns expose a clear imprint by the Galactic magnetic field leading to a narrow band of small dipole changes. Hereby, this pattern exposes the symmetry of the used magnetic field model. At $R = 1$ EV a

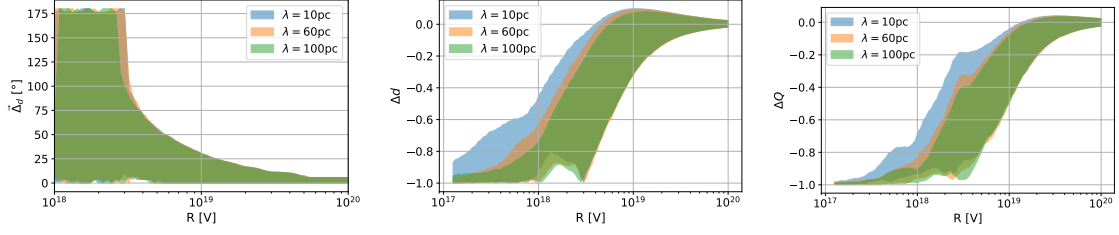


Figure 1. Range of the modification of the anisotropy as a function of the rigidity R . **Left:** Change of the dipole direction. **Middle:** Change of the dipole amplitude. **Right:** Change of the quadrupole amplitude.

dipole that points away from this narrow band has almost vanished, leading to some intriguing constraints on the maximal dipole amplitude as discussed in the following.

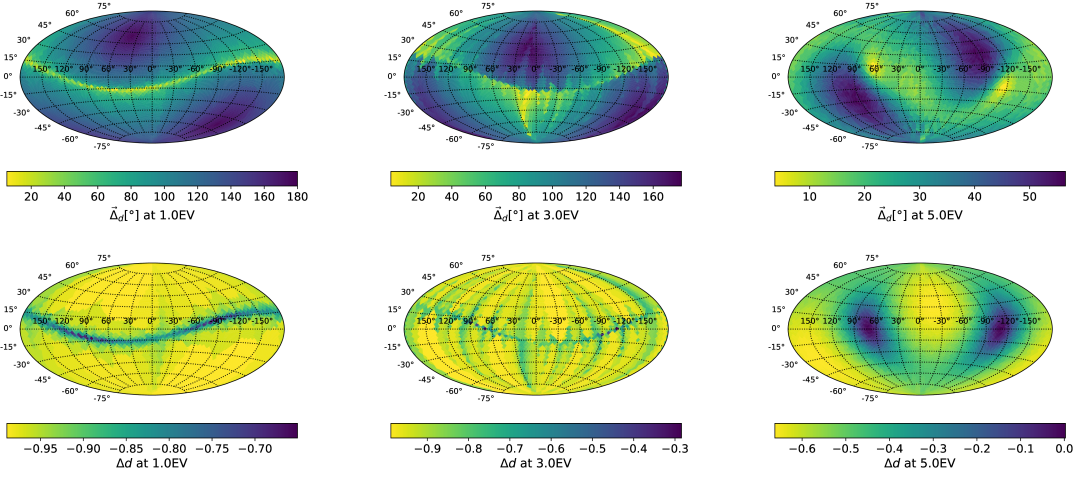


Figure 2. Modification of the dipole direction (**upper panel**) and amplitude (**lower panel**) dependent on its direction at Earth for three different CR rigidities using $\lambda = 60$ pc. Here and hereafter, the skyplots are displayed in Galactic coordinates.

We can determine the anisotropy amplitudes outside our Galaxy based on the observed amplitudes d_{obs} and Q_{obs} , respectively, according to

$$d_{\text{out}} = \frac{d_{\text{obs}}}{\Delta d + 1} \quad \text{and} \quad Q_{\text{out}} = \frac{Q_{\text{obs}}}{\Delta Q + 1}. \quad (3.1)$$

Note, that the corresponding change of the anisotropy direction is only taken into account for the dipole. Further, it needs to be satisfied that $d_{\text{out}}, Q_{\text{out}} \leq 1$. Therefore, we obtain a maximal dipole amplitude $\max(d_{\text{obs}}) = 1 + \Delta d$ at Earth dependent on the cosmic ray rigidity and the direction of the observed dipole. As indicated by the lower panel in Fig. 2, the suppression of the dipole amplitude at small rigidities is huge. E.g. there is a huge range of directions of the dipole where its observed amplitude at $R = 1$ EV cannot exceed $\sim 1\%$. At $R = 5$ EV this range of directions has become smaller, but still there are about two extended regions close to the Galactic center and its anti-center, where the dipole amplitude cannot exceed 34 %.

3.2 Total flux bias for a dipole anisotropy

Using the Eq. 3.1 we determine $(\Delta F)_d$ for an ideal observer as well as the difference $(\Delta F_{\text{Auger}} - \Delta F_{\text{TA}})_d$ between the different field of views of the observatories dependent on the observed direction and amplitude of the dipole anisotropy.

3.2.1 An ideal observer

Here, the left Fig. 3 shows the band of $(\Delta F)_d$, as the certain value depends on the direction of the dipole, in the case of a dipole anisotropy with three different amplitudes at Earth. At $R < 10$ EV the bands widen significantly and at certain rigidities we obtain a huge change of $(\Delta F)_d$ for certain dipole directions. The skyplots in the middle and right Fig. 3 reveal that these directions are about to correlate to the Galactic center and its anti-center. At small rigidities the pattern is almost symmetric in longitude, whereas at higher rigidities it becomes symmetric with respect to the galactic latitude.

Note that the unexpected increase of $(\Delta F)_d$ in the left Fig. 3 at small rigidities for a strong dipole amplitude d_{obs} is only an artifact of the constrain $d_{\text{out}} \leq 1$. Thus, at these rigidities the dipole directions of the maximal modification coincide with those where $\max(d_{\text{obs}})$ is smaller than the requested amplitude d_{obs} . In these cases we change d_{obs} to $\max(d_{\text{obs}})$, so that $d_{\text{out}} = 1$.

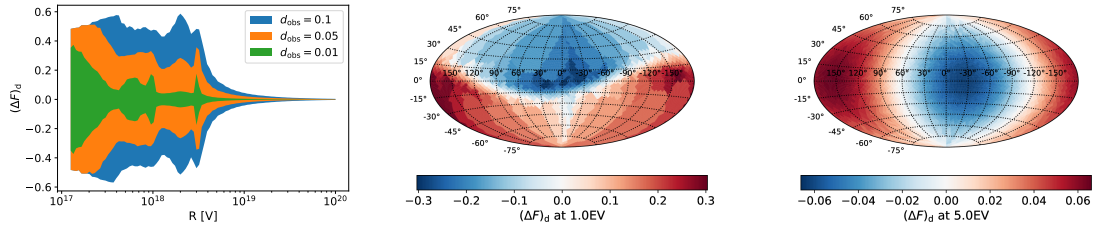


Figure 3. Modification of the UHECR flux due to a dipole anisotropy for an ideal observer. **Left:** Dependent on the rigidity. **Middle (right):** Dependent on the dipole direction using a CR rigidity of $R = 1$ EV ($R = 5$ EV) for an amplitude $d_{\text{obs}} = 0.05$ at Earth.

3.2.2 Difference between Auger and TA

In the following, we take the different field of views of the experiments into account and determine the flux difference between them. So, the bands of $(\Delta F_{\text{Auger}} - \Delta F_{\text{TA}})_d$ in the left Fig. 4 shows in principle a similar rigidity dependence as $(\Delta F)_d$ in the left Fig. 3. At $R \leq 1$ EV the bands for $d_{\text{obs}} \leq 0.05$ widen significantly with decreasing rigidity, so that even for a very small dipole amplitude a difference of more than 15% becomes possible for certain dipole directions. The directional pattern, as shown the middle and right Fig. 4, does not show any obvious correlation to the different field of views. Instead they reveal a similar directional pattern as in Fig. 3, hence, the directional dependence is less influenced by the different field of views than by the Galactic magnetic field.

In total, the Galactic magnetic field can lead to differences of more than 10% in the total flux that is observed by Auger and TA. However, the exact value strongly depends on the directions of the anisotropy, and the rigidity of the particle. To draw a conclusive answer on the UHECR flux modification by the Galactic magnetic field, we need to include the observed chemical composition as well as the direction of the dipole.

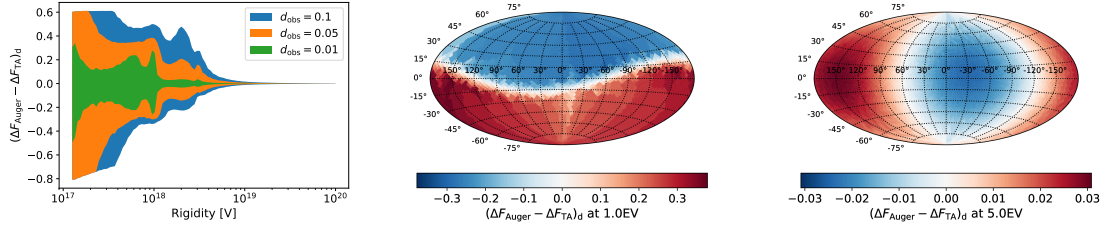


Figure 4. Difference of the UHECR flux due to a dipole anisotropy in the field of view of Auger and TA. The plot parameters and characteristics are the same as given in Fig. 3.

3.3 Total flux bias for a quadrupole anisotropy

In the case of the quadrupole anisotropy, we are unable to correlate the observed direction of the quadrupole to the one outside the Galaxy. Still we can provide the range of the bias based on the range of ΔQ , as given in the right Fig. 1. The left Fig. 5 shows that $(\Delta F)_q$ in the case of a symmetric quadrupole anisotropy yields a similar pattern as in the case of a dipole. However, the bands are no longer symmetric indicating that there are quadrupole directions that yield to a stronger amplification than suppression of the flux. Although, at certain rigidities, the suppression can still dominate. Further, there the bands show less peaks and the constrain $Q_{\text{out}} \leq 1$ applies even for $Q_{\text{obs}} = 0.01$ at small rigidities. On average the quadrupole anisotropy yields $(\Delta F)_q$ values that are a bit smaller than the $(\Delta F)_d$ values.

Further, the right Fig. 5 shows the corresponding flux difference $(\Delta F_{\text{Auger}} - \Delta F_{\text{TA}})_q$ between the field of view of Auger and TA. Interestingly, there is no general decrease of the magnitude of the differences between the two experiments, but the difference reaches a maximum at about 3 EV.

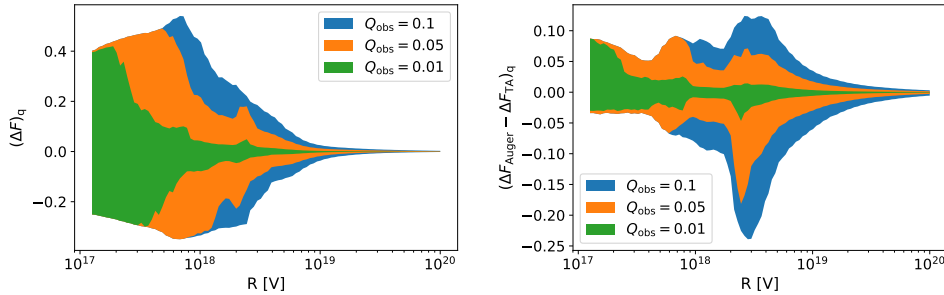


Figure 5. UHECR flux bias due to a quadrupole anisotropy. **Left:** For an ideal observer. **Right:** Difference between the field of view of Auger and TA.

4 Bias based on the Auger data

The relevance of the bias by the Galactic magnetic field considerably depends on the cosmic ray's rigidity and the direction of the anisotropy, as well as the magnetic field itself. Here, we use the JF12 model again with a coherence length of $\lambda = 60$ pc, unless otherwise stated. Further, we use the observed mean logarithm of the mass number $\langle \ln A \rangle$ [15], and the information on the dipole strength and direction [16] in the following to provide a constrain on this effect for the observed dipole anisotropy.

Table 1. Parameters of the Auger dipole.

E_{obs} [EeV]	d_{obs}	$(l, b)_{\text{obs}}$ [°]	$d_{\text{out},1}$	$d_{\text{out},2}$	$d_{\text{out},3}$	$(l, b)_{\text{out},1}$ [°]	$(l, b)_{\text{out},2}$ [°]	$(l, b)_{\text{out},3}$ [°]
5	0.032	(−73, −32)	0.183	0.057	0.051	(3, 0)	(−53, −57)	(−45, −51)
10.3	0.056	(−139, −3)	0.159	0.074	0.067	(−155, 14)	(−141, 7)	(−138, 5)
20.2	0.096	(−103, −34)	0.124	0.099	0.097	(−111, −45)	(−93, −42)	(−96, −39)
39.5	0.163	(−101, −11)	0.157	0.151	0.151	(−79, −17)	(−87, −14)	(−87, −14)

Here, $d_{\text{out},i}$ and $(l, b)_{\text{out},i}$ refer to the resulting dipole features outside our Galaxy using EPOS-LHC ($i = 1$), Sibyll2.1 ($i = 2$), and QGSJetII-04 ($i = 3$).

4.1 Total flux in case of the Auger dipole

The particle’s rigidity R_{obs} is approximated by

$$R_{\text{obs}} = \begin{cases} E_{\text{obs}}/(A/2), & \text{for } A \geq 2 \\ E_{\text{obs}}, & \text{for } A < 2, \end{cases} \quad (4.1)$$

where E_{obs} denotes the observed median energies of the dipole, as given in Table 1, and the mass number $A = \exp(\langle \ln A \rangle)$. Further, we use the derived power-law behavior of the dipole amplitude [16]

$$d_{\text{obs}} = 0.055 (E_{\text{obs}}/10 \text{ EeV})^{0.79} \quad (4.2)$$

and the observed directions $(l, b)_{\text{obs}}$ of the dipole — see Table 1. At energies that are not covered by the data of $\langle \ln A \rangle$ or $(l, b)_{\text{obs}}$ we use linear interpolation, where the boundary values are used outside the observed energy range. Since these data values can in principle change from outside our Galaxy to Earth, we use Δd dependent on $(l, b)_{\text{obs}}$ and R_{obs} in order to estimate the dipole outside our Galaxy dependent on the hadronic interaction model as listed in Table 1. Hereby, we also include the shift of the dipole direction due to the Galactic magnetic field. We suppose that neither the energy of UHECRs nor their chemical composition changes during the propagation through the Galaxy, which this is a necessary condition to apply the backtracking approach in the first place.

As shown in Fig. 6, the UHECR flux is reduced at energies $\ll 10$ EeV by several percentage — the exact value strongly depends on the hadronic interaction model — in the case of the observed dipole. Though, at about 10 EeV an amplification of at most 14% is obtained. As expected, the hadronic interaction model ‘EPOS-LHC’ [17, 18] that predicts the most heavy composition also leads to the largest values of ΔF . Further, the statistical uncertainties of $\langle \ln A \rangle$ as well as the directional uncertainty of the dipole direction lead to a wide range of ΔF values at a few EeV, in particular for the ‘EPOS-LHC’ model. Hence, at about 100 EeV, the flux can be amplified by 5 % or suppressed by more than 20%. Comparing this with the statistical uncertainty of the flux measurement of the Pierre Auger Observatory, which is between 0.5% and 5% below the cut-off at approx. 30 EeV, all model predictions lead to a significant total flux bias at about 3 and 5 EeV, respectively, at least.

The right Fig. 6 exposes that the previously described trend applies not only for Auger’s field of view but also for the common observation band of Auger and TA, i.e. $-15.7^\circ < \delta < 24.8^\circ$, as well as the ideal observer. In all cases the flux is amplified at about 10 EeV, but suppressed below and above this energy yielding a significant change of the spectral behavior in this energy range. At energies below some tens of EeV the observed flux is well described by a series of broken power laws [19], hence, $F_{\text{obs}}(E) \propto E^{-\alpha}$ yields $F_{\text{out}}(E) \propto E^{-\alpha+\Delta\alpha}$ outside the Milky Way as $F_{\text{out}} = F_{\text{obs}}(1 + \Delta F)^{-1}$. Due to the strong increase (decrease) of ΔF at

(5–10) EeV ((10–20) EeV), especially for the field of view of Auger, the spectral index differs by $\Delta\alpha \simeq -0.2$ ($\Delta\alpha \simeq 0.15$). Note that in the field of view of TA $\Delta\alpha$ is about a factor of two smaller. In general, both experiments underestimate the flux outside the Milky Way, except around 10 EeV where they overestimate it.³ Above 10 EeV this effect increases with energy and the spectral behavior of F_{out} becomes harder than the observed one. Comparing ΔF at energies < 10 EeV for Auger’s field of view with the one for TA’s field of view, the middle and right Fig. 6 expose that the flux suppression for Auger is up to (2–4) % larger than for TA. This can be compared to the approx. 10% difference between the full-Sky spectra measured by Auger and TA below the ankle [20]. In the common observation band the difference ($\Delta F_{\text{Auger}} - \Delta F_{\text{TA}}$) necessarily vanishes, but still there is a significant UHECR flux bias, in particular at some tens of EeV. However, the flux discrepancy between Auger and TA above 30 EeV can not be fully explained by the modification of the UHECR flux with the Galactic magnetic field model JF12. Note that the previously described effect of ΔF increases by about a factor of two in the case of $\lambda = 100$ pc.

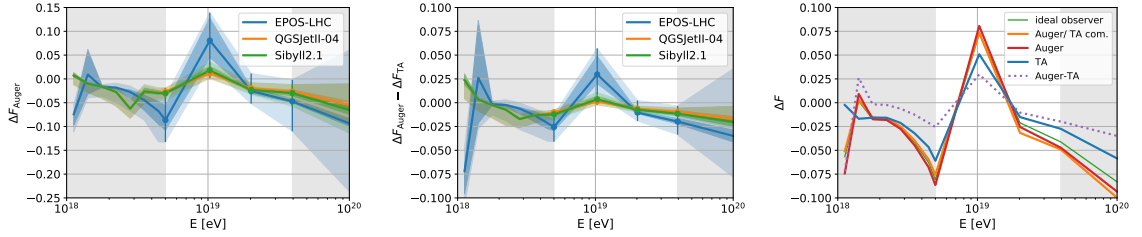


Figure 6. The UHECR flux bias and difference based on the Auger data using a coherence length of $\lambda = 60$ pc. Due to the lack of observational data, the dipole direction is not changed for $E < 5$ EeV and $E > 39.5$ EeV, which is indicated by the shaded background. **Left (middle):** The bias in Auger’s field of view (the difference between the field of view of Auger and TA) for three different hadronic interaction models. The statistical uncertainties of $\langle \ln A \rangle$ refers to the darker error band and the total error which includes the directional uncertainty of the dipole refers to the lighter band. **Right:** Using the hadronic interaction model ‘EPOS-LHC’ and the mean dipole direction, the bias is displayed for a full sky observatory (green line), Auger (red line), TA (blue line), the common observation band of Auger and TA (orange line), as well as the difference between Auger and TA (dotted purple line).

The directional dependence of ΔF_{Auger} , as given in Fig. 7, shows that a smaller longitude l of the observed dipole — within the range of the uncertainty — leads to a stronger suppression by about a factor of two, and vice versa in the case of the amplification at 10.3 EeV. In addition, the shift of the mean dipole direction by the Galactic magnetic field suggests that there are different source directions: At 5 EeV the dipole direction $(l, b)_{\text{out}}$ outside the Galaxy is likely close to the Galactic center, whereas at higher energies a rather high Galactic longitude is favored. In particular, at energies $E \geq 20$ EeV the dipole direction outside the Galaxy might stay the same if we account for the observational uncertainties. Note, that $(l, b)_{\text{out}}$ significantly depends on the used hadronic interaction model, especially at low energies, as shown in Table 1.

4.2 Constraints on the chemical composition

Using the constrain on the maximal dipole amplitude, i.e. $d_{\text{out}} \leq 1$, we use the Auger data of the observed dipole amplitude and the corresponding mean energy as given in Table 1,

³At about 1 EeV, they might also observe an amplified flux, but this depends strongly on the direction of the dipole at these energies which is currently not known.

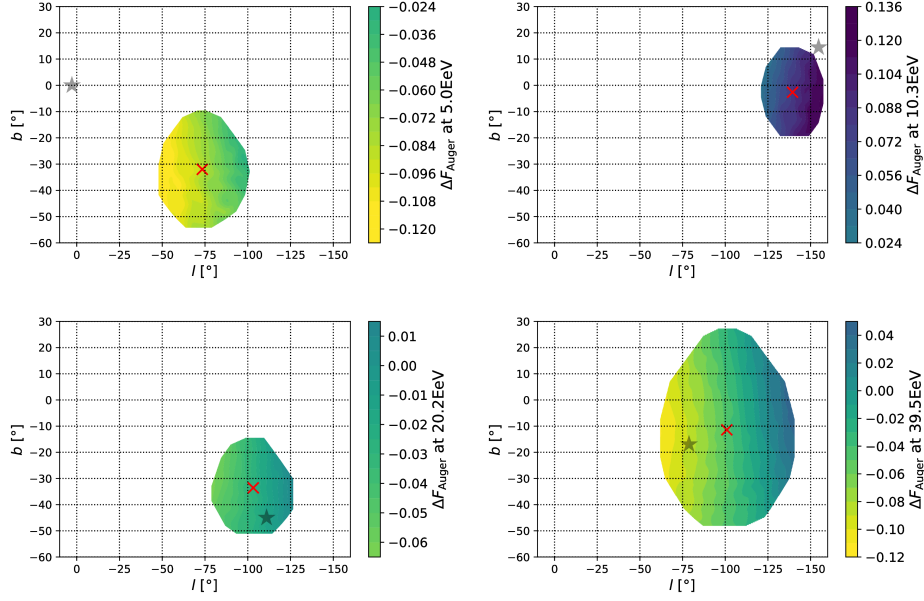


Figure 7. The directional dependence of the UHECR flux bias for Auger’s field of view. The red cross indicates the observed mean dipole direction and the black star refers to the corresponding dipole direction outside the Galaxy. Hereby, the hadronic interaction model ‘EPOS-LHC’ as well as a coherence length of $\lambda = 60$ pc has been used.

and determine the maximal mean charge number $\max(Z)$ dependent on the dipole direction. Hereby, we compute the necessary rigidity at the observed cosmic ray energies and dipole amplitudes in order to obtain $d_{\text{out}} \geq 1$. Fig. 8 indicates that the Galactic magnetic field yields an intriguing method to constrain the chemical composition of UHECRs for certain directions of the dipole that only depends on the Galactic magnetic field model and not on the hadronic interaction model. At low energies the observed dipole — in particular its mean direction — points towards a direction that constrains the maximal charge number of the UHECRs. Hence, for a coherence length of some tens of pc, the mean chemical composition at 5 EeV is at most constituted by CNO nuclei, whereas at 10 EeV and 20 EeV it could already be given by Si nuclei. Note, that in all cases the mean dipole direction is close to the narrow band that does not constrain the composition. Though, especially at 5 EeV the coherence length of the Galactic magnetic field changes this band, and for $\lambda = 100$ pc the constrain is significantly weakened. At the highest energies this method does not draw any constraints on the composition of UHECRs.

5 Conclusions

Using the Galactic lenses from the publicly available software package of CRPropa3, we investigated the impact of dipole and quadrupole anisotropies on the UHECR flux at Earth for the JF12 Model for the Galactic magnetic field. The flux modification ΔF in case of a quadrupole anisotropy is smaller by about a factor of two compared to the dipole anisotropy, however, the quadrupole amplitude is more reduced by the Galactic magnetic field than the dipole amplitude. Further, this effect allows to draw some compelling limits on the maximal observed amplitude of the anisotropy, in particular at small rigidities.

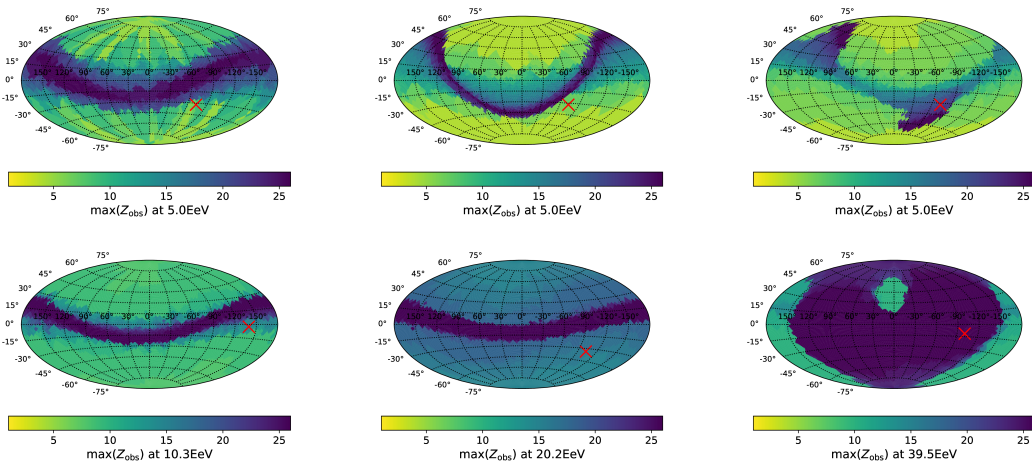


Figure 8. The maximal charge number of UHECRs dependent on the direction of the dipole. The red cross indicates the observed mean dipole direction by Auger. **Upper panel:** The dipole at 5 EeV using a coherence length of the Galactic magnetic field of $\lambda = 10$ pc (**left**), $\lambda = 60$ pc (**middle**) and $\lambda = 100$ pc (**right**). **Lower panel:** The dipole at higher energies using $\lambda = 60$ pc.

Considering the observed anisotropy level of a few percentages, it is shown that in general, a modification of the UHECR flux by more than 10% is possible for rigidities $R < 5$ EV and certain direction of the anisotropy, if we take the reduction of the anisotropy amplitude into account. Further, this modification by the Galactic magnetic field can in principle also produce differences in the measured UHECR spectrum of different experiments, and thus explain some of the differences between the measurements of the Auger and TA collaborations. Finally, we account for the observed chemical composition, as well as the observed dipole direction and amplitude, showing that the UHECR spectrum can be biased by more than 10% for the hadronic interaction model ‘EPOS-LHC’. Though, for all interaction models, this effect yields at a few EeV a suppression of the flux that is larger than the observational uncertainties. If we account for the observational uncertainties of the dipole direction, which allows directional shifts of several tens of degree, this effect can even be increased by about a factor of two. In total, this work demonstrates that the bias by the Galactic magnetic field impacts the interpretation of spectrum and composition data. So, it can lead to a suppression at the median energy of 5 EeV of up to 12% and an amplification at 10 EeV of up to 13%, which implies a change of the UHECR flux spectrum by $\Delta\alpha \simeq 0.2$ at most.

Further, we demonstrated that the amplitude and the mean energy of the observed dipole can be used to draw constraints on the maximal mean charge number of the UHECRs. Considering the mean direction again the charge number can be constrained to $Z \lesssim 7$ at 5 EeV, if the turbulent component of the Galactic magnetic field has a coherence length of about $\lambda = 60$ pc. Hence, if the UHECRs at this energy are on average composed of CNO nuclei there can only be a single dominant source outside the Galaxy. Otherwise the dipole amplitude $d_{\text{out}} \ll 1$, so that the amplitude at Earth $d \ll d_{\text{obs}}$. This consequence is in good agreement with previous investigations on the reduction of the degree of anisotropy by the JF12 model [21].

However, this effect does not fully resolve any of the discrepancies between the observations of different experiments, since the flux difference $(\Delta F_{\text{Auger}} - \Delta F_{\text{TA}})_d$ necessarily vanishes in the common observation band. Still, at several energies the bias ΔF can be at about the

same order as the reported difference in the case of a heavy composition of UHECRs.

It is intriguing that with the observed dipole some difference between the observed spectra of the experiments is expected. For updated dipole directions based on additional data, or the discovery of a significant quadrupole anisotropy, the Galactic magnetic field bias can become a major issue. Note, that these outcomes strongly depend on the used Galactic magnetic field model, and due to the current issues with this model, we strongly encourage to repeat this analysis with improved magnetic field models.

Acknowledgments

Some of the results in this paper have been derived using the software packages Numpy [22], Matplotlib [23] and HEALPix/ healpy [12]. TW acknowledges supported by DFG grant WI 4946/1-1.

References

- [1] L. A. Anchordoqui, *Ultra-High-Energy Cosmic Rays*, *Phys. Rep.* **801** (2019) 1–93, [[arXiv:1807.09645](#)].
- [2] **Pierre Auger** Collaboration, A. Aab et al., *Observation of a Large-scale Anisotropy in the Arrival Directions of Cosmic Rays above 8×10^{18} eV*, *Science* **357** (2017), no. 6537 1266–1270, [[arXiv:1709.07321](#)].
- [3] D. Harari, S. Mollerach, and E. Roulet, *Effects of the galactic magnetic field upon large scale anisotropies of extragalactic Cosmic Rays*, *JCAP* **1011** (2010) 033, [[arXiv:1009.5891](#)].
- [4] R. Jansson and G. R. Farrar, *A New Model of the Galactic Magnetic Field*, *Astrophys. J.* **757** (2012) 14, [[arXiv:1204.3662](#)].
- [5] M. C. Beck, A. M. Beck, R. Beck, K. Dolag, A. W. Strong, and P. Nielaba, *New constraints on modelling the random magnetic field of the MW*, *JCAP* **2016** (2016), no. 05 056, [[arXiv:1409.5120](#)].
- [6] J. L. Han, R. N. Manchester, W. van Straten, and P. Demorest, *Pulsar Rotation Measures and Large-scale Magnetic Field Reversals in the Galactic Disk*, *Astrophys. J. Suppl.* **234** (Jan, 2018) 11, [[arXiv:1712.01997](#)].
- [7] J. Xu and J. L. Han, *Magnetic fields in the solar vicinity and in the Galactic halo*, *Mon. Not. Roy. Astron. Soc.* **486** (2019), no. 3 4275–4289.
- [8] T. Winchen and B. Eichmann, *Modification of the Energy Spectrum of UHECR by the Galactic Magnetic Field for Anisotropic Arrival Directions*, in *36th International Cosmic Ray Conference (ICRC2019)*, vol. 36 of *International Cosmic Ray Conference*, p. 468, 2019.
- [9] The Telescope Array and Pierre Auger Collaborations, *Pierre Auger Observatory and Telescope Array: Joint Contributions to the 35th International Cosmic Ray Conference (ICRC 2017)*, 2018. [[arXiv:1801.01018](#)].
- [10] D. Harari, S. Mollerach, and E. Roulet, *The toes of the ultra high energy cosmic ray spectrum*, *Journal of High Energy Physics* **08** (1999) 22, [[astro-ph/9906309](#)].
- [11] H.-P. Bretz, M. Erdmann, P. Schiffer, D. Walz, and T. Winchen, *PARSEC: A Parametrized Simulation Engine for Ultra-High Energy Cosmic Ray Protons*, *Astropart. Phys.* **54** (2014) 110–117, [[arXiv:1302.3761](#)].
- [12] K. M. Górski et al., *HEALPix: A Framework for High-Resolution Discretization and Fast Analysis of Data Distributed on the Sphere*, *Astrophys. J.* **622** (2005) 759–771, [[astro-ph/0409513](#)].

- [13] R. Alves Batista et al., *CRPropa 3 - a Public Astrophysical Simulation Framework for Propagating Extraterrestrial Ultra-High Energy Particles*, *JCAP* **1605** (2016) 038, [[arXiv:1603.07142](#)].
- [14] P. Sommers, *Cosmic ray anisotropy analysis with a full-sky observatory*, *Astroparticle Physics* **14** (2001), no. 4 271–286, [[astro-ph/0004016](#)].
- [15] **Pierre Auger** Collaboration, A. Aab et al., *Depth of Maximum of Air-Shower Profiles at the Pierre Auger Observatory. I. Measurements at Energies above $10^{17.8}$ eV*, *Phys. Rev. D* **90** (2014) 122005, [[arXiv:1409.4809](#)].
- [16] **Pierre Auger** Collaboration, A. Aab et al., *Large-scale cosmic-ray anisotropies above 4 EeV measured by the Pierre Auger observatory*, *Astrophys. J.* **868** (2018), no. 1 4, [[arXiv:1808.03579](#)].
- [17] T. Pierog and K. Werner, *Muon Production in Extended Air Shower Simulations*, *Phys. Rev. Lett.* **101** (2008) 171101, [[astro-ph/0611311](#)].
- [18] T. Pierog, I. Karpenko, J. M. Katzy, E. Yatsenko, and K. Werner, *EPOS LHC: Test of Collective Hadronization with Data Measured at the CERN Large Hadron Collider*, *Phys. Rev. C* **92** (2015) 034906, [[arXiv:1306.0121](#)].
- [19] **Pierre Auger** Collaboration, V. Verzi, *Measurement of the energy spectrum of ultra-high energy cosmic rays using the Pierre Auger Observatory*, in *36th International Cosmic Ray Conference (ICRC2019)*, vol. 36 of *International Cosmic Ray Conference*, p. 450, Jul, 2019. [[arXiv:1909.09073](#)].
- [20] T. AbuZayyad et al., *Auger-TA energy spectrum working group report*, *EPJ Web of Conferences* **210** (2019) 01002.
- [21] G. R. Farrar and M. S. Sutherland, *Deflections of UHECRs in the galactic magnetic field*, *Journal of Cosmology and Astroparticle Physics* **2019** (2019), no. 05 004–004.
- [22] S. van der Walt, S. C. Colbert, and G. Varoquaux, *The NumPy Array: a Structure for Efficient Numerical Computation*, [[arXiv:1102.1523](#)].
- [23] J. D. Hunter, *Matplotlib: A 2D Graphics Environment*, *Comput. Sci. Eng.* **9** (2007), no. 3 90–95.